Development of a parallel CFD code for modeling steady laminar axisymmetric non-premixed co-flow flames with soot

Zhang, A. Q.; Thomson, M. J.; Guo, Hongsheng; Liu, Fengshan; Smallwood, Gregory

Publisher's version / Version de l'éditeur:

2007 Combustion Institute/Canadian Section (CI/CS) Spring Technical Meeting. Session G: Fires and Flames (Numerical Studies) [Proceedings], 2007

DEVELOPMENT OF A PARALLEL CFD CODE FOR MODELING STEADY LAMINAR AXISYMMETRIC NON-PREMIXED CO-FLOW FLAMES WITH SOOT

A. Q. ZHANG, M. J. THOMSON
and
H. GUO[†], F. LIU[†], G. J. SMALLWOOD[†]
Department of Mechanical and Industrial Engineering, University of Toronto, Canada
[†]ICPET, National Research Council, Canada

INTRODUCTION

Most of the world's heat and power is generated by the combustion of various fossil fuels such as coal, gasoline and diesel. Combustion is a complex multi-physics phenomenon which involves heat and mass transfer, chemical kinetics, thermodynamics and fluid dynamics. When considering soot formation, the complexity is greatly enhanced by other simultaneous processes such as aerosol dynamics (i.e. nucleation, growth, coagulation and oxidation) and radiation heat transfer [1]. In order to gain a detailed understanding of the soot processes, the soot model discussed in this paper uses a detailed, fundamental approach to solve the above mentioned processes. For example detailed chemical kinetics and multi-section aerosol dynamics with particle clusters are implemented in this paper.

Implementing detailed multi-physics phenomena in a model comes at a large computational cost. The authors started with a sequential FORTRAN 77 code for modeling the steady laminar axisymmetric co-flow non-premixed flames [2]. The run time to get the converged solution with a chemical mechanism of 36 species is about a week on a desktop computer [2]. However, with (1) more complex chemical mechanisms such as the Appel mechanism with 101 species and 543 reactions [3]; or (2) larger geometry and more grid points needed to well resolve the computational domain; or (3) complex physical problems such as the soot formation with sectional representation, the computational time becomes excessive. This motivated the authors to choose parallel computation to speed up the calculations so that more complex problems can be investigated within a reasonable amount of time.

MODELING TECHNIQUE AND PARALLELIZATION METHODOLOGY

Mathematical Representation and Numerical Methods

The fully elliptic governing equations for conservation of mass, axial and radial momentum, gas species mass fractions, sectional soot quantities and energy in cylindrical coordinate system and the boundary conditions form a closed system. The governing equations are solved using the pressure correction method in the segregated manner. Due to the limited space, these equations are not shown here. The reader is referred to [2] for additional details. The diffusive terms are discretized by the central difference scheme while the convective terms are discretized by first order upwind scheme. Soot nucleation, growth and oxidation are modeled by the Fairweather

model [4]. The aerosol dynamics of soot particles are modeled by the Fixed-Sectional Representative-Size approach [5]. To model the formation of soot clusters, two equations --- (1) the number density of clusters and (2) the number density primary particles --- are solved in each section. The numerical procedure to solve the system is summarized in Fig. 1. Since the flame is axisymmetric, only half of the vertical cross sectional plane is employed as the computational domain to save computational time.

Parallelization Methodology

In this study, Message Passing Interface (MPI) is chosen as the parallel development tool since it is widely used and easy to program. After a careful analysis of the sequential code, it is found that an elegant way to parallelize the code is via Domain Decomposition Method (DDM). By DDM, the whole computational domain is divided into Nprocesses sub-domains, Nprocesses being the number of Processes used. Communications are needed for the sub-domain boundary points. Ghost points are placed in the boundary of each sub-domain to minimize the information exchange rate. Fig. 2 shows an example of the computational domain decomposed with 5 Processes. Since the flame is modeled under cylindrical coordinate system, the domain is decomposed in the axial direction only. This way, the parallel coding is much easier since the radial variable declarations are the same as the sequential code and thus not needed to be modified. In Fig.2, strips of different colors are the sub-domains and the numbers represent individual Processes responsible for the computation of that sub-domain.

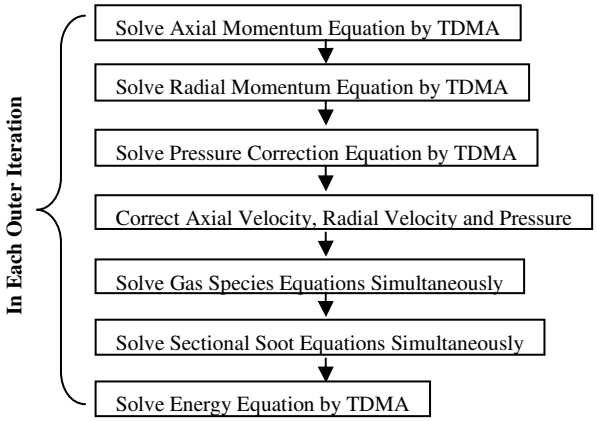

(TDMA: Tri-Diagonal Matrix Algorithm)

Fig.1 Numerical Procedure

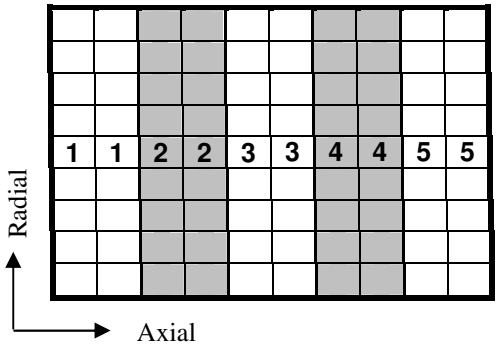

Fig. 2 Example of 5 Processes Used to Decompose the Computational Domain

RESULTS AND DISCUSSION

Validation of Parallel Code

The parallel code is employed to model a lightly sooting methane flame which has been studied by Smooke [6] and Liu [7]. The computational conditions in this study are the same as those assumed by Smooke. The burner fuel tube has an inner radius of 0.5556 cm and the wall thickness is 0.0794 cm. Both the oxidizer (air) and fuel (methane) inlet velocities and temperatures are assumed to be uniform, i.e. VF=5.52 cm/sec, VA=12.54 cm/sec, TF=TA=420 K. The chemical kinetic mechanism used in this calculation is GRI-Mech 3.0 with the removal of all reactions and species related to NO_x formation and contains 36 species. The chemical reaction

rates, thermal and transport properties are obtained by CHEMKIN subroutines. Non-uniform mesh is used in both axial and radial directions to save computational time while resolving the large gradients. The computational domain covers 8.655 cm (axial, Z direction) × 4.709 cm (radial, R direction) and is divided into 192(Z) × 86(R) control volumes. Fine grids were placed in the R direction between 0 and 0.75 cm with a grid resolution of 0.2 mm and in the Z direction between 0 and 2.95 cm with a grid resolution of 0.2 mm. Beyond the fine grid zone, the mesh is gradually stretched with a stretch ratio of 1.07 in the Z direction and 1.05 in the R direction. It has been checked that further refinement of the mesh has negligible impact on the predicted results. Inlet conditions are specified for the fuel and air streams at the Z = 0 boundary. Symmetry conditions were enforced at the centerline, i.e., R = 0. Free-slip conditions are assumed for the velocity at the axial out boundary (i.e. at R=4.709 cm). Zero-gradient conditions are enforced at the exit boundary. The radiation by gaseous species CO_2, H_2O and CO is calculated by Optically Thin Assumption (OTA) model. 35 sections are used to resolve the size distribution of soot particles with a section spacing factor of two. The first section soot particles are assumed to contain 90000 carbon atoms. The resulting system is a set of 110 equations (1+1+1+36+35×2+1) to be solved in each control volume. The calculation was performed on the NRC ICPET cluster which is comprised of AMD Opteron™ 64bit Redhat Linux machines with the Portland Group PGI 6.2 FORTRAN compiler and MPI library.

Radial Temperature Profile at Different Heights above the Burner

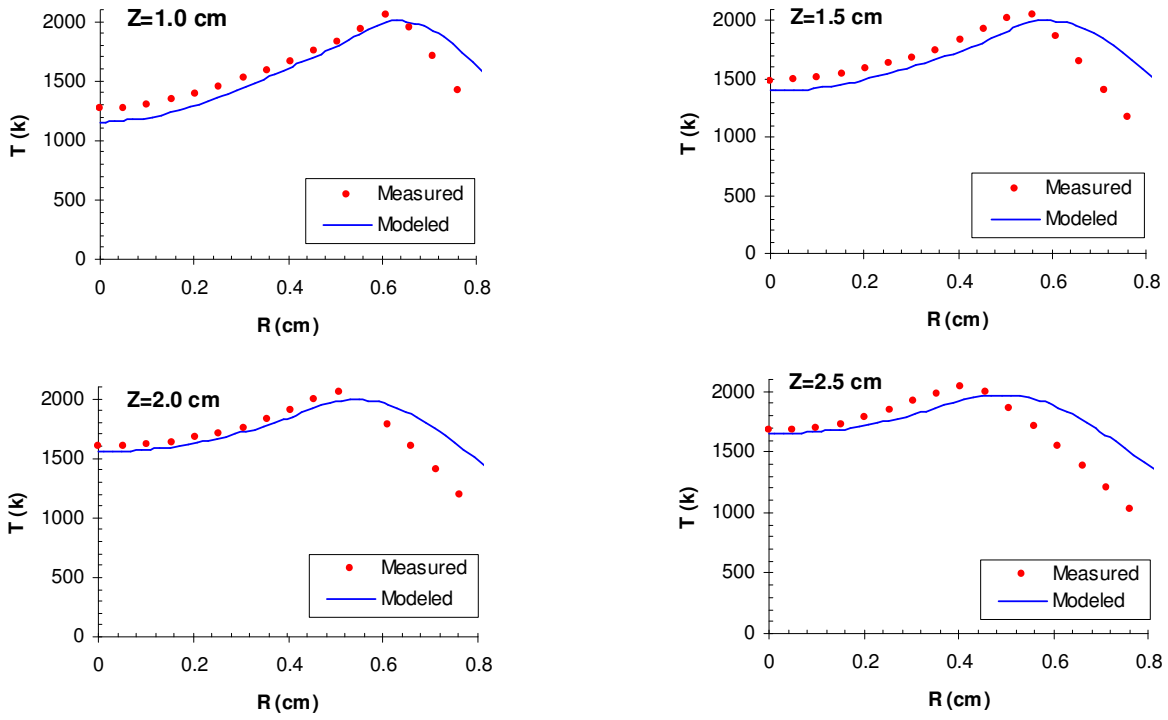

Fig. 3 Radial Temperature Profile at Different Heights above the Burner

From Fig. 3, it can be found that this model predicts the flame temperatures reasonably well. The peak flame temperature appears in the flame wing instead of the centerline. At 1.0 cm above the burner (Z=1.0 cm), the centerline temperature is underpredicted by about 100K. However, as Z

increases, the centerline temperature is predicted better. At Z=2.5 cm, the predicted centerline temperature is about 25 K lower than the experimental one. The lower predicted centerline temperature may be attributed to the uncertainties in the inlet condition and the simplified radiation model. Except for Z=2.5 cm, the radial locations of the peak temperature are considered to be well predicted. As R increases from zero (i.e. the centerline) to the radial peak temperature locations, this model underpredicts the temperature. Beyond the radial peak temperature locations, the predicted temperatures do not fall off as fast as the measured temperatures and thus are overpredicted. However, overall, the temperature field is well predicted.

Flame Height

Fig. 4 shows the centerline temperature against the height above the burner. According to Smooke [6], a good estimate of the flame height is the location of the peak centerline temperature. It can be found from Fig.4 that T peaks at about Z=4.05 cm which is very close to the experimental visible flame height of 4.1 cm [7].

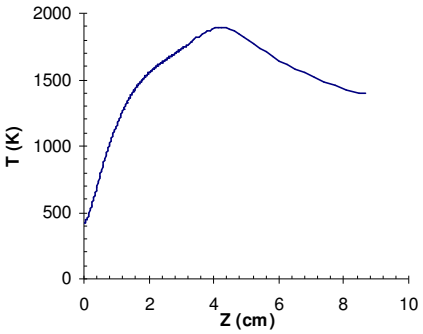

Fig. 4 Centerline Temperature vs. Height above Burner

Radial Acetylene Profile at Different Heights above the Burner

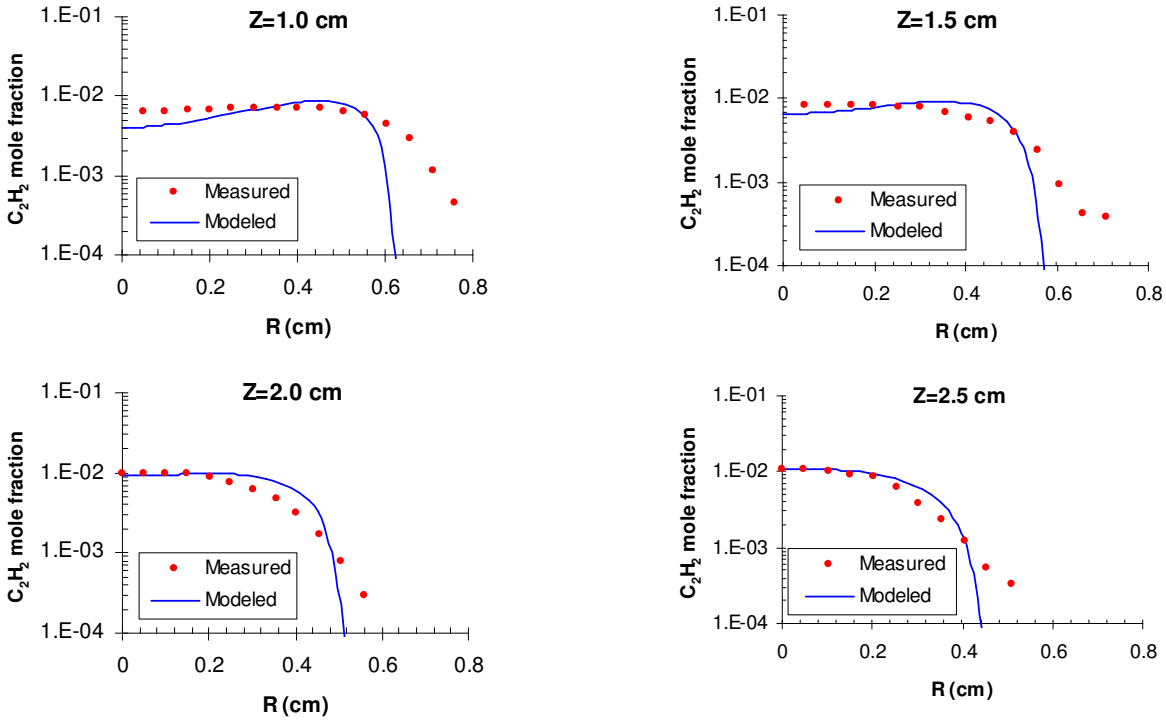

Fig. 5 Radial Acetylene Profile at Different Heights above the Burner

It can be found from Fig. 5 that this model predicts well the general trend of the acetylene levels. This model underpredicts the centerline acetylene levels. This may be due to the underprediction of centerline flame temperature. Also, it should be noted that this model predicts sharper decay of acetylene levels in the outer radial region. This is due to the overprediction of the temperature in these regions.

Radial Soot Volume Fraction Profile at Different Heights above the Burner

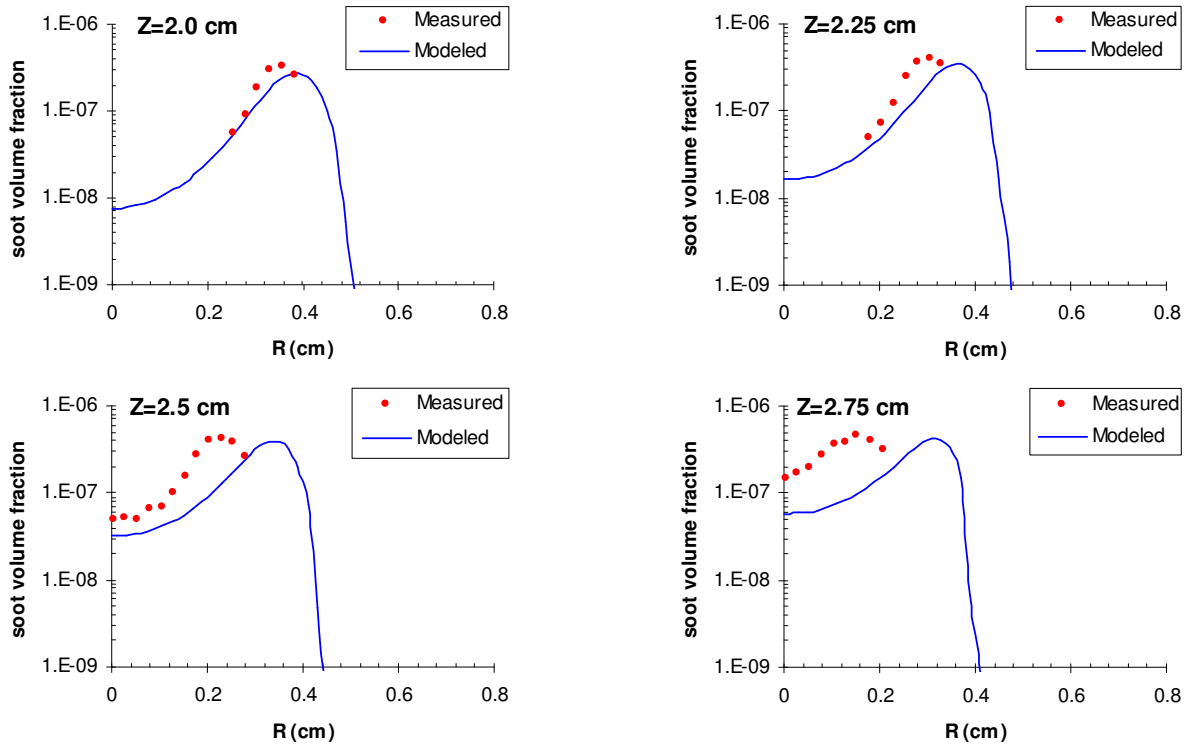

Fig. 6 Radial Soot Volume Fraction Profile at Different Heights above the Burner

It can be found that although there are some discrepancies between the prediction and measurement, this model generally well predicts the trend and absolute level of soot volume fraction. The predicted peak soot volume fraction is 4.2E-7 and the measured peak is 4.7E-7. Such a small difference again confirms the good predictability of the soot volume fraction field of the present model. Fig. 7 shows the 2D contour plot of the predicted soot volume fraction field. The soot peaks in the wing of the flame which agrees with Smooke [6] and Liu [7].

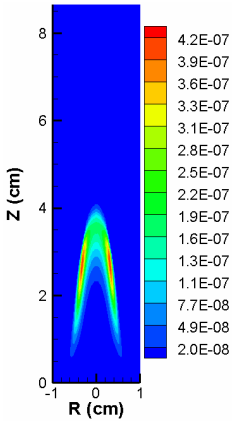

Fig. 7 2D Representation of Soot Volume Fraction

PARALLEL CODE PERFORMANCE ANALYSIS

In order to analyze the performance of the parallel code, 1 (which is essentially sequential), 4, 6 and 12 Processes are used to run the code respectively. The CPU time to get the converged solution are compared. And the Speedup curve is shown in Fig. 8. Speedup is defined by the ratio of sequential code CPU time to parallel code CPU time.

The Speedup curve can be linearly fitted to Speedup=0.8×Nprocesses+0.16. It can be seen that such Speedup is sub-linear, i.e. the slope is less than unity. This is due to the overhead associated with the transfer of information among different Processes in the calculation and, to a less extend, the sequential property of the TDMA solver. Nevertheless, the Speedup scales quite well with the number of Processes with 0.8 being the scaling coefficient. Such efficiency is considered to be good.

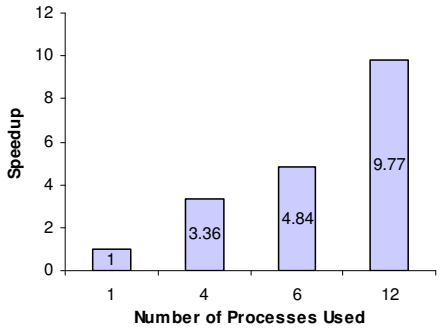

Fig. 8 Speedup under Different Processes

CONCLUSIONS

A parallel computational fluid dynamics code for modeling steady laminar axisymmetric non-premixed co-flow sooting flames is developed using domain decomposition method. The code is then employed to model an experimental sooting methane flame using the GRI-Mech 3.0 chemical mechanism. Results show that the parallel code can well predict the flame temperature, flame height, major species and soot volume fraction in such flame. Comparison of the CPU time of the sequential and parallel codes using the same chemical mechanism shows that a good parallel efficiency is achieved.

ACKNOWLEDGEMENTS

AUTO21 is acknowledged for the financial support. S.H. Park and S. Rogak are acknowledged for the help with the sectional aerosol dynamics model. And R. Jerome is acknowledged for the help with the NRC ICPET cluster.

REFERENCES

1. Smooke, M.D., Long, M.B., Connelly, B.C., Colket, M.B. and Hall, R.J., Combust. Flame 143:613 (2005).
2. Guo, H., Liu, F., Smallwood, G. J. and Gulder, O.L., International Journal of Computational Fluid Dynamics 18 (2):139 (2004).
3. Appel, J., Bockhorn, H., and Frenklach, M., Combust. Flame 121:122 (2000).
4. Fairweather, M., Jones, W.P., Lindstedt, R.P., Combust. Flame 89:45 (1992).
5. Wen, J.Z., Thomson, M.J., Lightstone, M.F., Rogak, S.N., Energy & Fuels 20:547 (2006).
6. Smooke, M.D., McEnally, C.S., Pfefferle, L.D., Hall, R.J. and Colket, M.B., Combust. Flame 117:117 (1999).
7. Liu, F., Guo, H., and Smallwood, G. J. Combust., Flame 138:136 (2004).